

DragonClaw: A low-cost pneumatic gripper with integrated magnetic sensing

Vani H. Sundaram, Raunaq Bhirangi, Mark E. Rentschler, Abhinav Gupta, and Tess Hellebrekers

Abstract— Advances in robotics and rapid prototyping have spurred interest in soft grippers across diverse fields ranging from medical devices to warehouse robotics. With this growing interest, it is imperative to create straight-forward soft grippers with embedded sensing that are more accessible to people outside of the soft robotics community. The DragonClaw — a 3D-printable, pneumatically actuated, three-fingered dexterous gripper with embedded magnetic tactile sensing — is intended to bridge this gap. The 2-DOF thumb design allows for a range of precision and power grasps, enabling the DragonClaw to complete a modified Kapandji test for dexterous ability. The operating range of the gripper is characterized through experiments on grip strength and finger blocking force. Further, the integrated magnetic sensor, ReSkin, is successfully demonstrated in a closed-loop control task to respond to external disturbances. Finally, the documentation, bill of materials, and detailed instructions to replicate the DragonClaw are made available on the DragonClaw website, encouraging people with wide ranging expertise to reproduce this work. In summary, the novelty of this work is the integration of soft robotic gripper feedback in a form factor that can easily be reproduced by inexpensive, simplified manufacturing methods.

I. INTRODUCTION

Soft robotics research has been exponentially growing, with the general goal of improving safety, adaptability, and versatility of robots. Conventional robots can perform a wide range of difficult precision tasks; however, they require intricate mechanical designs and kinematic control to safely conform to its environment due to their rigid nature [1]. While rigid grippers are extremely effective for well-defined tasks, they do not generalize across large groups of objects, respond to unexpected disturbances, or present easy to replicate designs [2]. In contrast, soft robotic grippers are cheaper, compact, and reliable. They offer simplified mechanical and control systems for dexterous manipulation of objects of variable size, shape, weight, and hardness [3]. Due to their innate compliant properties, soft grippers are more effective than traditional grippers when dealing with delicate objects, environmental disturbances, and uncertainty [4].

Despite the promising performances of many soft grippers that exist in literature, several lack the successful integration of sensors, which hinders a device's ability to interact with its environment. A number of works have demonstrated

V.H. Sundaram and M.E. Rentschler are with the Department of Mechanical Engineering, University of Colorado Boulder, Boulder, CO 80309 USA (e-mails: vani.sundaram@colorado.edu, mark.rentschler@colorado.edu).

R. Bhirangi is with Carnegie Mellon University and Meta AI Research

A. Gupta is with Carnegie Mellon University

T. Hellebrekers is with Meta AI Research

Vani H. Sundaram is the corresponding author for this work (e-mail: vani.sundaram@colorado.edu).

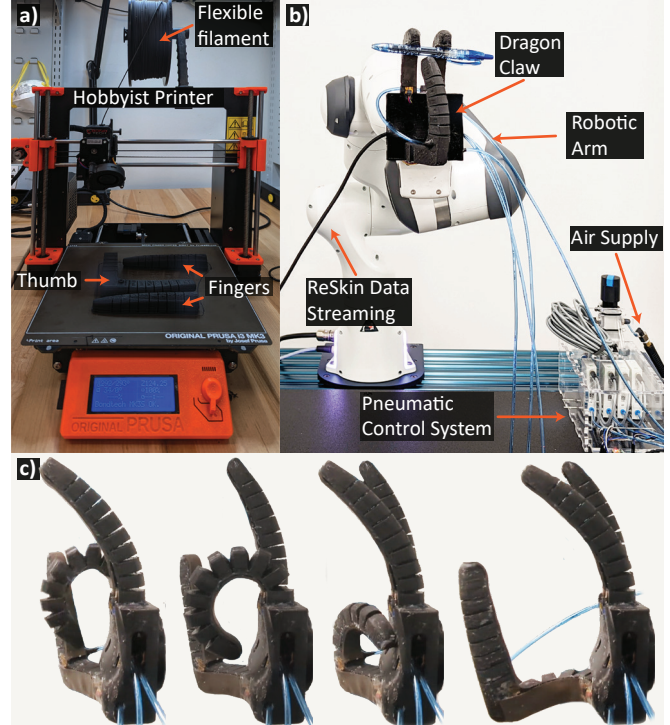


Fig. 1: a) All digits can be printed in 18 hrs using a commercial printer and flexible filament with a 75A shore hardness. b) The full setup up of the DragonClaw mounted on a commercial robotic arm. The ReSkin sensor data was streamed via USB to the main computer. The pneumatic control system and air supply are housed in an external container; the maximum input pressure of 200 kPa was controlled by a filter regulator and independently distributed to each channel shown in c) through four proportional pressure regulators. c) The four channels that can be controlled are the pointer, middle, thumb, and palm (from left to right). These are all at 100% actuation (200 kPa) .

successful open-loop control of soft grippers when handling fragile objects [5], [6], [7]. However, the viability and adaptability of soft robotic grippers is fully actualized by integrating sensing systems for feedback control. On-board sensors allow grippers to register their own state [8], [9] and actively adapt to environmental stimuli using closed-loop control [10], [11]. Most effective among these are embedded soft sensors that conform to the soft actuator's movement without limiting its performance. Unfortunately, while soft grippers with embedded sensing are well-placed to resolve the above limitations, in practice, the design and integration is not trivial.

Adoption of soft gripper and sensing technology has long been sluggish due to the expensive equipment, complex manufacturing procedures, and a lack of extensive back-

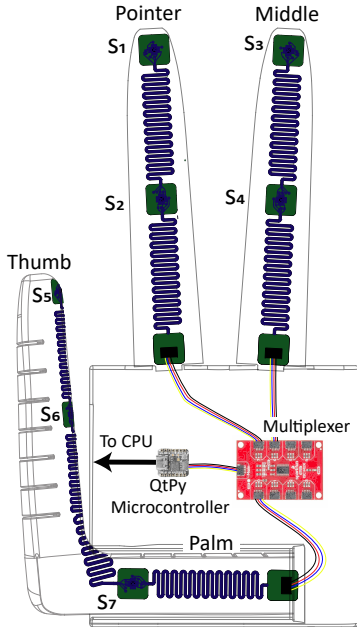


Fig. 2: The pointer and middle fingers each have two sensors, one at the fingertip (s_1 and s_3 , respectively) and one positioned at the center of each finger (s_2 and s_4 , respectively). The thumb has three sensors, one at the fingertip (s_5), one at the center of the thumb (s_6), and one on the “palm-side” of the thumb (s_7). The sensor strands are all connected to a multiplexer and communicate over I2C bus, which is connected to a microcontroller. The microcontroller then sends data to the main computer via USB.

ground experience. [12], [13], [14]. Recently, researchers have been able to leverage advances in rapid prototyping and additive manufacturing [15], [16], [17] technologies, unlocking the potential for developing soft grippers and fabrication procedures that are inexpensive and accessible all types of researchers.

To that end, we created DragonClaw – a soft robotic gripper with integrated sensing that can be assembled with off-the-shelf parts and a 3D printer. This simple, 3-fingered design allows for both opposition and reposition movements (Fig.1c), increasing the diversity of available grasps and hand positions, like the tripod pinch-grasp shown in Fig.1b. This gripper includes seven magnetic-based sensors, or ReSkin[18], which we use to understand the deformation of each finger and react to external disturbances while completing a task. We use the sensors to control both the DragonClaw’s fingers and the pose of a commercial robotic arm. The overall cost of creating and using the sensorized DragonClaw is detailed and included as open-sourced documentation, available on the project’s website. The DragonClaw aims to strike a balance between ability and simplicity to encourage collaborative community growth.

II. RELATED WORK

A. Manufacturing Methods

Soft grippers that actuate based on positive pressure inputs have been extensively studied in the field, with a specific focus on pneumatic networks. Researchers have tried different materials [19], [20], designs [21], [9], analytical models [22],

[5], and manufacturing methods [23], [24] to improve soft pneumatic actuators for grippers. There has been a shift away from the traditional molding method of creating pneumatic networks because it is a time-consuming, multi-step process that becomes more involved with complex actuator designs [25], [9]. To address this issue of complicated manufacturing techniques, researchers are using additive manufacturing techniques to simplify the process. This allows for easier, iterative design and fabrication processes [17]. Many groups that 3D print their actuators use expensive commercial printers [26] or modified printers [27], which can be difficult for a broader audience to access. With the DragonClaw, we aim to alleviate this lack of accessibility by leveraging a common 3D printer and filament for the fabrication of the entire gripper.

B. Integrated Tactile Sensing

Embedded sensors allow soft actuators, and therefore grippers, to properly interact with their environment and measure its own state. Rocha et al. designed and characterized the use of both resistive and capacitive pressure sensors [28]. The resistive sensors were embedded into the fingertips of a soft robotic gripper, and they were used when performing a series of grasping tasks to demonstrate the sensor performance. Some groups like Shorthose et al. designed a 3-D printed, anthropomorphic gripper with fully embedded sensing [10]. They utilized the pressure differences in the printed sensing regions distributed across the hand to determine applied pressure and location of pressure. Jamil et al. embedded optical sensors in a pneumatic gripper to measure the bending deformations and contact force for each actuator [29]. While these sensors are very effective, they require complicated system integration processes or are prone to hysteresis effects. To address this, we chose to incorporate ReSkin – a magnetic sensing technology that is easy to integrate, provides accurate and precise distributed sensing, is less susceptible to hysteresis effects, and enables multi-axis force sensing [18]. Additionally, ReSkin does not require a direct electrical connection between the circuitry and the soft magnetic interface, which makes the system inherently more robust and less restricting to the movement of the gripper.

C. Important Contributions

These prior actuators and grippers demonstrate the benefits of using additive manufacturing and utilizing embedded sensing, but have yet to show a gripper that 1) demonstrates dexterous movements, 2) uses embedded sensors in a closed-loop system to adapt to external disturbances, and 3) lowers the barrier to entry for new researchers. Here, we utilize a standard 3D printer and commercially available material to create air-tight pneumatic actuators, which we use in a three-fingered gripper. We design a thumb that can demonstrate several power and precision grasps. For the integrated sensing method, we chose to use ReSkin, a magnetic-based tactile sensor developed by Hellebrekers et al. [30], [18], and we successfully used these sensors to control the movement of the gripper when a disturbance is introduced.

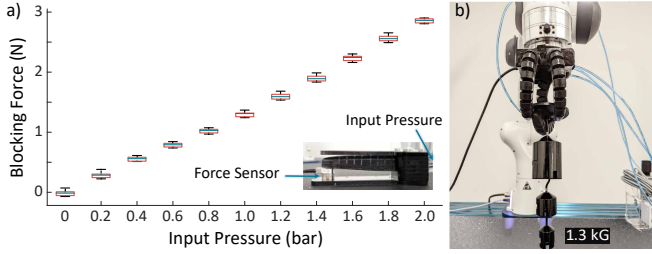


Fig. 3: a) The image at the bottom right shows the experimental setup used to test the blocked force of the finger. The base of the finger was secured to the fixture and the tip of the finger was aligned over the center of a force sensor. As the pressure increased from 0-200 kPa (0-2 bar), the blocking force proportionally increased to a max of 3 N. Each box plot shown represents the force distributions for the four trials run for six different actuators (24 trials at each pressure). The center line represents the median, the box outlines the interquartile range, and the horizontal lines show the minimum and maximum force values of those 24 trials. b) The maximum grip strength of the DragonClaw was determined to be 1.3 kg.

III. HAND AND INTEGRATED SENSING DESIGN

A. Hand and Actuation Circuit Design

The DragonClaw was designed based on three main criteria: 1) easily accessible to novice researcher, 2) successful execution of both the pinch and power grasps, and 3) integration of tactile sensing across the palm-side of the gripper. The first criterion encourages a broader audience to leverage this technology, to reduce the barrier of entry to compliant robotic manipulation and propel related research work forward. The power and pinch grasp requirements serve to demonstrate the effectiveness of the thumb design, since the thumb accounts for 60% of hand functionality [31]. While embedding sensors in the gripper is optional, the integrated sensing allows us to demonstrate the DragonClaw's ability to adapt to environmental changes and not just complete repetitive tasks.

TABLE I: Cura Slicer Printing Settings

Quality	
Layer Height	0.25 mm
Line Width	0.4 mm
Walls	
Wall Thickness	0.8 mm
Wall Line Count	2
Top/Bottom	
Top Layers	15
Bottom Layers	12
Infill	
Infill Density	30%
Infill Pattern	Lines
Material	
Printing Temperature	227 °C
Final Printing Temperature	220 °C
Build Plate Temperature	50 °C
Speed	
Print Speed	13 mm/s
Infill Speed	10 mm/s
Wall Speed	12 mm/s
Inner Wall Speed	12 mm/s
Top/Bottom Speed	10 mm/s
Travel	
Enable Retraction?	Yes
Retraction Distance	0.5 mm
Retraction Speed	10 mm/s
Cooling	
Enable Print Cooling?	Yes
Support	
Generate Support?	Yes
Support Placement	Touching Buildplate

We used a Prusa i3 MK3S+ printer (Prusa Research) with a modified extruder (Bondtech Mini Gear extruder upgrade, Bondtech) to print the fingers and thumb (setup shown in Fig. 1a). As denoted in Table II, the type of printer and the extruder replacement are optional; we chose the Prusa i3 MKS+ because it is a common, hobbyist-level printer and the Bondtech extruder because the filament feeding mechanism is preferred when using soft filament. The material used was a flexible, thermoplastic elastomer (TPE) (Chinchilla 75A, NinjaTek). We used Ultimaker Cura 5.0.0 to slice the 3D model using the settings shown in Table I. Printing two fingers and a thumb took 18 hours and 27 minutes to print using these settings and printing hardware.

The finger design was based on the design described in Hainsworth et al. [16] to minimize the bending stiffness, improve the range of motion of the fingers, and eliminate inter-layer air leaks. The specific settings outlined in Table I are critical to avoid leaks in the fingers when fully actuated. It is also important to note that if the manufacturing equipment hardware outlined in Table II changes, then these settings will need to be tweaked accordingly. The material settings should remain relatively constant. Each finger has one degree-of-freedom (DOF); the thumb was designed to have two DOF, linear abduction and adduction motion in addition to interphalangeal (IP) flexion, which we refer to as the palm motion. This palm design is similar to that in Deimal and Brock's pneumatic hand [32] - our palm motion allows for opposability, which is shown in 4.

We used a Fused Deposition Modeling (FDM) printer (Stratasys Fortus 450mc, Stratasys) with acrylonitrile butadiene styrene (ABS) material (ABS-M30, Stratasys) to print the palm. This combination of printer and material is optional for the palm; any printer than with the ability to add rigid, removable supports will be sufficient. This design requires supports because it is a hollow design with several curved surfaces to fit the electrical components into the palm.

The pneumatic control system outlined in Table II and shown in Fig. 1 is composed of commercially available proportional pressure control valves VEABs with the ability to finely adjust the input pressure to the actuators (Festo Co.). The pressure regulators used for this study had a pressure range of 0-200 kPa, so the filter regulator was capped at 200 kPa. The air compressor stayed at a constant 800 kPa. These components make up a significant amount of the total cost, but alternative brands can be used as a more cost-effective substitute. We chose to purchase these specific components to allow for more fine-tuned control of the pressure input to each finger.

There was one VEAB for each DOF in the hand, and each VEAB was independently controlled using analog outputs from a microcontroller (Teensy 4.0, PJRC). The VEAB ran on a 0-10 V input, which linearly scaled to a 0-200 kPa pressure output. Since the Teensy 4.0 can only output a maximum of 3.3 V, we used a non-inverting operational amplifying (Op-Amp) circuit to scale the 0-3.3 V signal to a 0-10 V signal. The true pressure value was recorded through the VEAB by the Teensy at 100 Hz, where the 0-10 V output

TABLE II: Cost of System Parts

Item	Recommended Part and Brand	Price
<i>Manufacturing Equipment</i>		
3D Printer Extruder*	Prusa i3 MK3S+* Bondtech BMG Prusa Extruder*	\$799 \$110
<i>Manufacturing Materials</i>		
Filament Palm Silicone Glue	NinjaTek Chinchilla FDM using ABS-M30 Stratasys* Sil-Poxy Smooth-On	\$11.86 \$32.00 \$3.30
<i>Sensor Components*</i>		
Magnetic Microparticles	MQP-15-7 Magnequench	\$30.00
Magnetization Process	Magnet-Physiks*	\$44.00
Silicone	Dragon Skin 20 Smooth-On	\$4.83
Planetary mixer*	AR310 Thinky*	\$11,000.00
Degasser*	Bel-Art™ Space Saver Vacuum Desiccators*	\$190.10
Vacuum*	ZENY Economy Vacuum Pump*	\$71.98
Sensor MCU	QT Py - SAMD21 Dev Board Adafruit	\$7.50
Multiplexer	Qwiic Mux Breakout - 8 Channel Sparkfun	\$12.95
Connectors	Flexible Qwiic Cable - 100mm	\$6.40
Flexible Sensor Boards	Full Assembly PCBWay	\$152.90
Magnetometers	MLX90393 Melexis*	\$13.79
<i>Electronic Components</i>		
Pneumatic Controller MCU	Teensy 4.0 PJRC	\$22.80
Pneumatic Controller Circuit	SMT Assembled PCBWay	\$145.66
<i>Pneumatic Control System</i>		
Proportional Pressure Regulator(4)	8046305 FESTO*	\$2428.88
Tube Fittings(5)	QSY-4 FESTO*	\$21.60
Filter Regulator	529166 FESTO*	\$137.60
Tubing 4mm Diameter	8048671 FESTO*	\$20.00
Air Compressor	Stealth Ultra Quiet Air Compressor*	\$229.00
Equipment Investment:		\$18,145.13
Material Investment:		\$529.59
Sensor Costs:		\$11,534.45
Total:		\$15,496.15

* Indicates that this component and/or brand is optional

signal from the VEAB was scaled down to a 0-3.3 V signal using a voltage divider.

B. Integrated Tactile Sensing

While soft grippers are compliant and naturally conform to surrounding objects and obstacles, embedded sensing allows for more informed reactions in response to environmental changes. For this gripper, we used ReSkin [18], [30], which is a soft, inexpensive, easy-to-manufacture sensor with 3-axis signal output and high temporal resolution. The sensing component of DragonClaw is an optional addition, but it enables the ability to react to external stimuli and adapt accordingly, as shown in Section V.

The manufacturing process of the ReSkin used for this work closely follows the process described in Bhirangi et al [18]. We mixed bonded neo powder (MQP-15-7, Magnequench) and a 2-part polymer (Dragonskin, Smooth-On) using a 2:1:1 ratio. After a few rounds of hand-stirring, we placed the mixture in a planetary mixer for 30 s clockwise, immediately followed by 30 s counter-clockwise. We then poured the mixture into a 1.0 mm thick mold and removed the air bubbles using a vacuum chamber. To quickly cure the sample, we placed the mold in an oven at 50 °C for 1-1.5 h. If a planetary mixer and vacuum chamber are not accessible, then the hand-stirring step can be completed for a longer period of time and the air bubble removal step can be done using a concentrated heat source, like a hairdryer. Unlike

previous work, the magnetization process was outsourced to Magnetic-Physiks Inc. after fully curing. However, this step can also be performed using one or two strong magnets [18], [30].

Building upon previous work in using a magnetic sensing mechanism to measure changes in deformation of a soft robotic platform, we implemented magnetometers in each finger and the thumb [34]. Each finger had two magnetometers (MLX90393, Melexis) each and the thumb had three sensors, all facing the palm-side as shown in Fig. 2. The circuit boards for all three digits were thin, flexible circuits (PCBWay): they did not affect the strain-limiting layer of each digit. The three flexible circuit boards were connected to a multiplexer (TCA9548A, SparkFun) using 4-pin cables (Qwiic Cables, SparkFun) and communicated with a microcontroller (QTPy SAMD21 Dev Board, Adafruit) using I2C communication. A computer sampled the USB streamed sensor data at 360 Hz, which included a timestamp, temperature for all seven sensors, and 3-axis magnetic flux readings for all seven sensors. The multiplexer and the microcontroller, along with the associated wires, were housed in the palm (see Fig. 2).

The magnetized sample was cut to the shape of each finger. We then glued both the flexible sensor circuit and the magnetized sample to each finger using a silicone glue (Sil-Poxy, Smooth-on). Since the thumb had the two different strain limiting layers for each degree-of-freedom, we glued

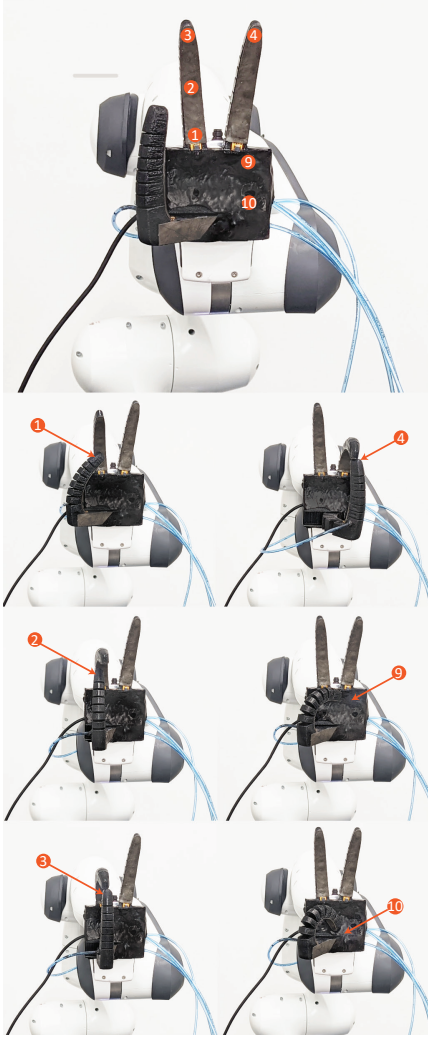


Fig. 4: We modified the traditional 10-position Kapandji test to accommodate a 3-finger gripper. This included the equivalent of 1) the lateral side of the second phalanx of the index finger, 2) the lateral side of the third phalanx, 3) the tip of the index finger, 4) the tip of the middle finger, 9) thumb on the proximal crease of the little finger, and 10) thumb on the distal volar crease of the hand [33].

the sensor circuit onto the thumb so that two sensors sat on the inner thumb and the third sensors sat on the palm-portion of the thumb (refer to Fig. 2). Then, we place two separate magnetized samples on each of the thumb’s strain limiting layers.

C. Resources

The 3D-printer, filament, slicer software, and modified extruder are all available commercial products. The setup steps and printer settings are available for download on the project website. The circuit board design and parts list for the pneumatic valves and sensing are available on the project website. The optional ReSkin sensing is, at this time, still required to be mixed and cured in a lab, though all materials (silicone and powder) are commercially available and magnetization may be outsourced.

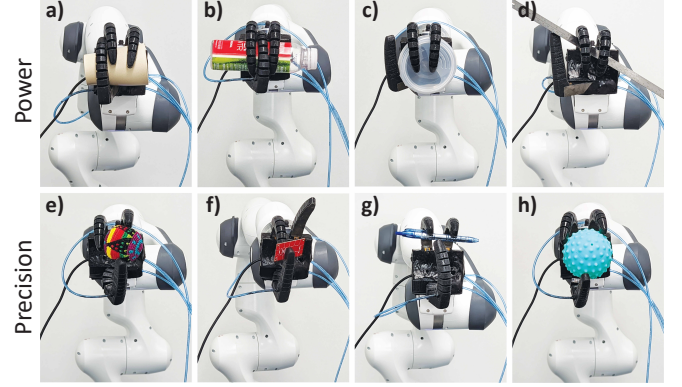


Fig. 5: a-d) Demonstrate power grasps and e-h) demonstrate precision grasps. These eight grasp postures were picked from the GRASP taxonomy to show the level of dexterity that DragonClaw exhibits. All objects were placed except those in a), f), and h), which picked up the respective objects from a surface (shown in Fig. 6).

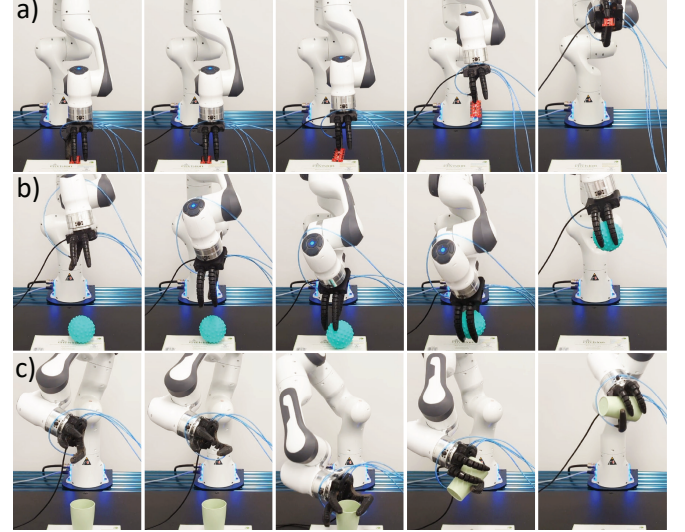


Fig. 6: a) The tip pinch grasp, b) the precision sphere grasp, and c) the medium wrap grasps are shown from picking up a thin, rectangular object and holding the object for 30 s to ensure object stability. The second frames in a-c) show the actuation of the palm to change the placement of the thumb.

IV. FINGER AND HAND CHARACTERIZATION

First, we characterize the relationship between blocking force and input pressure for the 3D-printed pneumatic fingers. Next, we measure the maximum holding force for a static weight placed in the gripper. Lastly, we highlight the gripper’s dexterity through a Kapandji test, modified for only three fingers. Altogether, the blocking force of a finger, grip strength of the hand, and qualitative dexterity observations provide good starting guidelines for characterizing this robot gripper design.

A. Strength Tests

It is critical to understand the strength of the gripper to determine advantages and constraints of the hardware. To understand the capabilities of DragonClaw, we needed to measure: 1) the blocking force of a single finger, where the elongation of the actuator is restricted, with respect to the input pressure, and 2) the maximum weight that the

DragonClaw could successfully hold. Fig. 3 a) shows the blocking force throughout the range of input pressure for six different finger samples. Each finger was mounted to an apparatus with a clamp for the base of the finger and a force sensor (F/T Sensor: Nano17, ATI Industrial Automation) placed under the fingertip. Then, the pressure input increased by 20 kPa every 2 s from 0-200 kPa. This test was run four times per finger across six individual samples, and the full force distribution of the 24 tests at each pressure input step are shown in Fig.3a).

We also performed a discrete weight test to measure the grip strength of the DragonClaw. To complete this test, we printed a 1 mm thick disc with a 100 mm diameter using PLA on a Prusa. The disc had an 85% infill to ensure structural integrity of the disc once a weight was attached. A small u-hook was attached to the disc using two M3 bolts. The DragonClaw was attached to a Franka Arm and positioned about 300 mm from the surface, palm parallel to the surface. The disc was handed off to the DragonClaw in a power grip, where all the fingers are fully contracted (200 kPa). We used a set of weights (10-1000 g Weight Set, HomeScienceTools) and slowly added weights at 10 g increments onto the disc. After adding each new weight, the DragonClaw must securely hold the weights for 30 s to be considered a success. Fig.3b) shows the final successful round, for a final maximum hold weight of 1.3 kg. The following round failed at 1.4 kg.

B. Dexterity Tests

The Kapandji test outlines the ten positions for a hand with four fingers and a thumb to demonstrate opposability [33]. We adapted this test for a hand with two fingers and one thumb, as shown in Fig.4. The six positions that we attempted were equivalent to these motions for a human hand: 1) the lateral side of the second phalanx of the index finger, 2) the lateral side of the third phalanx, 3) the tip of the index finger, 4) the tip of the middle finger, 9) thumb on the proximal crease of the little finger, and 10) thumb on the distal volar crease of the hand. The four positions that we excluded require positions on fingers that the DragonClaw does not have (the ring and pinky fingers). The DragonClaw was successfully able to complete the modified Kapandji test.

The Feix GRASP taxonomy describes 33 different grasps for a variety of different objects to demonstrate the dexterity of a five-fingered hand [35]. We picked four power grasps and four precision grasps that were compatible with a three-fingered hand and showed a wide-range of grasping techniques. The medium wrap, small diameter, power disk, and light tool grasps (Fig.5a)-d), respectively) are all power grasps; and the tripod, tip pinch, prismatic three-finger, and precision sphere grasps (Fig.5e)-h), respectively) are all precision grasps. While most of these objects were placed, the medium wrap, tip pinch, and precision sphere grasp-objects were all picked up from a surface by the robot arm. These three grasp demonstrations are shown in the supplementary video and in Fig.6.

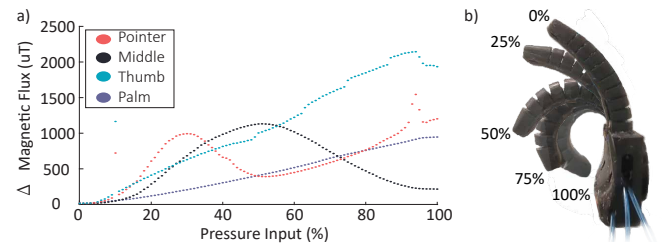


Fig. 7: a) The sensor data shows the average change in magnetic flux magnitude ΔB (μT) of all the sensors on the three digits, and the ΔB for the sensor on the palm. b) The movement of the middle finger at different input pressures.

V. DEMONSTRATIONS AND DISCUSSION

After the design, manufacturing, and characterization of the DragonClaw, we want to highlight the ability of the fully-integrated system. DragonClaw benefits from integrated magnetic sensing, which moves the system towards closed-loop control and a sufficient understanding of its own state and external environment.

A. Pressure Feedback

The dynamic output of the sensors gives us information about the deformation of each finger based on the input pressure to each channel. This information can be used to control the shape of the DragonClaw to produce grip positions like those shown in Fig. 5 using a closed-loop system, allowing the DragonClaw to properly interact with its environment. To understand the sensor output based on input pressure, we measured the change in magnetic field, ΔB , for each of the sensors as the three digits went from fully resting (0 kPa) to fully actuated (200 kPa). We linearly increased the input pressure in steps of 1% from 0% to 100%, where 100% represents the maximum 200 kPa pressure input and a 1% increment is equivalent to a 20 kPa increase. Each pressure step was held for 2 s before the next increase to ensure a steady pressure input and sensor output reading. Each of the four pressure channels were actuated individually, as shown in Fig.1c). The average magnitude of the 3-axis ΔB for the sensors on each finger is shown in Fig. 7. The sensors on the fingers and thumb can measure the change in pressure; however, the changes registered by the palm sensor are less well-defined. We believe this is due to the single sensor on the palm and the reduced range of motion in the palm compared to the fingers and thumb. Additionally, there's a nonlinear relationship between the pressure input and sensor output for the fingers, which we believe is caused by the non-uniform magnetic profile of the ReSkin. To address this in the future, we intend to uniformly magnetize the ReSkin.

B. Human-in-the-Loop Sensor Feedback

The integrated sensing allows the DragonClaw to respond to changes in the environment in ways that external sensors, like cameras, would not detect. To demonstrate this adaptability, we consider a human interaction where a user tries to remove an item from the robot's grasp. The DragonClaw was attached to a Franka Panda Arm; we used Polymetis [36] for real-time robot control based on the sensor inputs. The

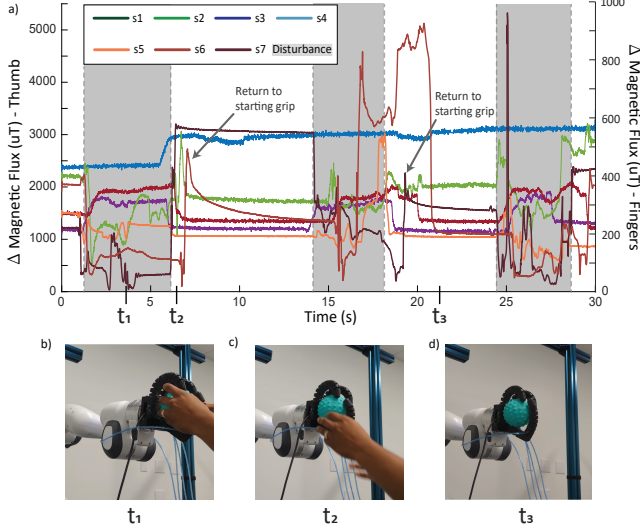


Fig. 8: a) Sensor output over time during human-in-the-loop interaction while robot maintains grip on the object. The time points marked on the graph correspond visually to when b) pressure is maxed out, c) the arm starts to move back, d) and adjusts grip to the resting grip position.

pressure inputs, in percent pressure of the maximum 200 kPa input, for the pointer finger, middle finger, thumb, and palm are $[p_1, p_2, p_3, p_4]$, respectively (labeled in Fig. 8a).

The DragonClaw started off with a loose grip on the ball (see Fig. 8), which required a [40%,40%,40%,50%] input. The palm was at a 50% input to position the thumb in the center of the point and middle fingers, stabilizing the grip on the ball. We kept the loose grip as the baseline grip, instead of a full power grasp, to give the system some range to strengthen its grip as needed. A 40% input to the fingers and thumb was the minimum pressure input needed to maintain a stable grip on the ball.

We applied a disturbance force to the ball by pulling the ball away from the hand in various directions. As the sensors on a finger measured an increase in the rate of change of magnetic flux $\dot{\mathbf{B}}$, the pressure input for that finger also increased. For example, if the two sensors on the thumb measured an increase in $\dot{\mathbf{B}}$, then p_3 increased accordingly; once $\dot{\mathbf{B}}$ was below a $5000 \mu\text{T}/\text{s}$ threshold, p_3 stopped increasing. If the pressure was at 100% and $\dot{\mathbf{B}}$ was still increasing, then the robot arm moved back until the disturbance force was removed. The removal of the disturbance force was marked by the sensor readings being within a $100 \mu\text{T}$ range of the baseline sensor readings when loosely grasping the ball. Once the disturbance force was fully removed, the robot arm moved back to the resting position with a loose grasp on the ball. Figure 8 outlines a summary of these results, showing the success of the DragonClaw adapting to random environmental disturbances. In this case, the disturbance was caused by the user trying to remove a ball from the hand's grasp, and the successful outcome was the DragonClaw tightening its grip until it reached the maximum pressure input before triggering the backwards movement of the robotic arm.

VI. CONCLUSIONS AND FUTURE WORK

This work describes the process of creating a DragonClaw: an accessible soft gripper design with integrated sensing. This gripper costs approximately \$500 USD for the materials and, despite only having 4 pressure input channels to two fingers and a thumb, it demonstrates opposability and dexterity. It can handle objects of varying weight, shape, and size and use closed-loop controlled movements to adapt to environmental disturbances. DragonClaw aims to keep manufacturing and accessibility to novice researchers as a priority, leveraging hobby-level 3D printing and printable parts. While we chose to use more expensive pneumatic components, fabrication methods for making ReSkin, and printer extruder (92% of the total cost) to ensure fine-tuned control and repeatable manufacturing outcomes, this is not a requirement and can be replaced by components that are a fraction of the price. The simple and effective design of this gripper lowers the barrier to entry for anyone who is interested in using this technology.

The demonstrations shown in this work showcase the capabilities of the DragonClaw; however, there are several improvements that can be made to the next iteration. Currently, the on-board sensing is sparse and cannot fully cover the palm. Adding more sensors to the DragonClaw would enable precise sensing capabilities over the entire surface of the hand, similar to a human hand. Additionally, the design of the thumb was simplified to only require two pressure inlets, in order to minimize start-up cost. However, this limits the full range of motion of the thumb, so future iterations could add more DOFs to the thumb and the palm.

ACKNOWLEDGMENTS

Vani H. Sundaram's contributions were supported in part by the National Science Foundation under Grant No. 1739452. We also thank Michael Fraser (fingers), Nicole Evans (palm), Steven Bain (FESTO), and Joel Gordon (MatterHackers) for their guidance and help.

REFERENCES

- [1] J. Shintake, V. Cacucciolo, D. Floreano, and H. Shea, "Soft Robotic Grippers," *Advanced Materials*, vol. 30, no. 29, p. 1707035, 2018. eprint: <https://onlinelibrary.wiley.com/doi/pdf/10.1002/adma.201707035>.
- [2] D. Arulkirubakaran, R. Malkiya Rasalin Prince, R. Ramesh, T. C. S. N. Rajesh, K. Neil Anand, S. M. Mathew, S. T. Baby, J. Anila Sharon, and K. C. S. Kishore, "Evolution of Industrial Robotic Grippers—A Review," in *Recent Advances in Materials and Modern Manufacturing* (I. A. Palani, P. Sathiya, and D. Palanisamy, eds.), Lecture Notes in Mechanical Engineering, (Singapore), pp. 553–563, Springer Nature, 2022.
- [3] C. Laschi, B. Mazzolai, and M. Cianchetti, "Soft robotics: Technologies and systems pushing the boundaries of robot abilities," *Science Robotics*, vol. 1, p. eaah3690, Dec. 2016. Publisher: American Association for the Advancement of Science.
- [4] S. Kim, C. Laschi, and B. Trimmer, "Soft robotics: a bioinspired evolution in robotics," *Trends in Biotechnology*, vol. 31, pp. 287–294, May 2013.
- [5] G. Gu, D. Wang, L. Ge, and X. Zhu, "Analytical Modeling and Design of Generalized Pneu-Net Soft Actuators with Three-Dimensional Deformations," *Soft Robotics*, vol. 8, pp. 462–477, Aug. 2021. Publisher: Mary Ann Liebert, Inc., publishers.

- [6] Y. Ye, P. Cheng, B. Yan, Y. Lu, and C. Wu, "Design of a Novel Soft Pneumatic Gripper with Variable Gripping Size and Mode," *Journal of Intelligent & Robotic Systems*, vol. 106, p. 5, Aug. 2022.
- [7] D. Bauer, C. Bauer, A. Lakshminipathy, R. Shu, and N. S. Pollard, "Towards very low-cost iterative prototyping for fully printable dexterous soft robotic hands," in *2022 IEEE 5th International Conference on Soft Robotics (RoboSoft)*, pp. 490–497, 2022.
- [8] H. Yang, Y. Chen, Y. Sun, and L. Hao, "A novel pneumatic soft sensor for measuring contact force and curvature of a soft gripper," *Sensors and Actuators A: Physical*, vol. 266, pp. 318–327, Oct. 2017.
- [9] S. Dilibal, H. Sahin, J. O. Danquah, M. O. F. Emon, and J.-W. Choi, "Additively Manufactured Custom Soft Gripper with Embedded Soft Force Sensors for an Industrial Robot," *International Journal of Precision Engineering and Manufacturing*, vol. 22, pp. 709–718, Apr. 2021.
- [10] O. Shorthose, A. Albini, L. He, and P. Maiolino, "Design of a 3d-printed soft robotic hand with integrated distributed tactile sensing," *IEEE Robotics and Automation Letters*, vol. 7, no. 2, pp. 3945–3952, 2022.
- [11] M. Tavakoli, P. Lopes, J. Lourenço, R. P. Rocha, L. Giliberto, A. T. de Almeida, and C. Majidi, "Autonomous Selection of Closing Posture of a Robotic Hand Through Embodied Soft Matter Capacitive Sensors," *IEEE Sensors Journal*, vol. 17, pp. 5669–5677, Sept. 2017. Conference Name: IEEE Sensors Journal.
- [12] A. D. Marchese, C. D. Onal, and D. Rus, "Autonomous Soft Robotic Fish Capable of Escape Maneuvers Using Fluidic Elastomer Actuators," *Soft Robotics*, vol. 1, pp. 75–87, Mar. 2014. Publisher: Mary Ann Liebert, Inc., publishers.
- [13] B. Mosadegh, P. Polygerinos, C. Keplinger, S. Wennstedt, R. F. Shepherd, U. Gupta, J. Shim, K. Bertoldi, C. J. Walsh, and G. M. Whitesides, "Pneumatic Networks for Soft Robotics that Actuate Rapidly," *Advanced Functional Materials*, vol. 24, pp. 2163–2170, Apr. 2014. Publisher: John Wiley & Sons, Ltd.
- [14] H. Lipson, "Challenges and Opportunities for Design, Simulation, and Fabrication of Soft Robots," *Soft Robotics*, vol. 1, pp. 21–27, Mar. 2014. Publisher: Mary Ann Liebert, Inc., publishers.
- [15] H. K. Yap, H. Y. Ng, and C.-H. Yeow, "High-Force Soft Printable Pneumatics for Soft Robotic Applications," *Soft Robotics*, vol. 3, pp. 144–158, Sept. 2016. Publisher: Mary Ann Liebert, Inc., publishers.
- [16] T. Hainsworth, L. Smith, S. Alexander, and R. MacCurdy, "A fabrication free, 3d printed, multi-material, self-sensing soft actuator," *IEEE Robotics and Automation Letters*, vol. 5, no. 3, pp. 4118–4125, 2020.
- [17] G. D. Goh, G. L. Goh, Z. Lyu, M. Z. Ariffin, W. Y. Yeong, G. Z. Lum, D. Campolo, B. S. Han, and H. Y. A. Wong, "3d printing of robotic soft grippers: Toward smart actuation and sensing," *Advanced Materials Technologies*, vol. 7, no. 11, p. 2101672, 2022.
- [18] R. Bhirangi, T. Hellebrekers, C. Majidi, and A. Gupta, "ReSkin: versatile, replaceable, lasting tactile skins," in *Proceedings of the 5th Conference on Robot Learning*, pp. 587–597, PMLR, Jan. 2022. ISSN: 2640-3498.
- [19] J. Shintake, H. Sonar, E. Piskarev, J. Paik, and D. Floreano, "Soft pneumatic gelatin actuator for edible robotics," in *2017 IEEE/RSJ International Conference on Intelligent Robots and Systems (IROS)*, pp. 6221–6226, Sept. 2017. ISSN: 2153-0866.
- [20] N. Elango and A. A. M. Faudzi, "A review article: investigations on soft materials for soft robot manipulations," *The International Journal of Advanced Manufacturing Technology*, vol. 80, pp. 1027–1037, Sept. 2015.
- [21] W. Hu, W. Li, and G. Alici, "3D Printed Helical Soft Pneumatic Actuators," in *2018 IEEE/ASME International Conference on Advanced Intelligent Mechatronics (AIM)*, pp. 950–955, July 2018. ISSN: 2159-6255.
- [22] J.-Y. Lee, J. Eom, S. Y. Yu, and K. Cho, "Customization Methodology for Conformable Grasping Posture of Soft Grippers by Stiffness Patterning," *Frontiers in Robotics and AI*, vol. 7, 2020.
- [23] R. Mutlu, C. Tawk, G. Alici, and E. Sarıyıldız, "A 3D printed monolithic soft gripper with adjustable stiffness," in *IECON 2017 - 43rd Annual Conference of the IEEE Industrial Electronics Society*, pp. 6235–6240, Oct. 2017.
- [24] A. D. Marchese, R. K. Katzschnmann, and D. Rus, "A Recipe for Soft Fluidic Elastomer Robots," *Soft Robotics*, vol. 2, pp. 7–25, Mar. 2015. Publisher: Mary Ann Liebert, Inc., publishers.
- [25] M. S. Xavier, C. D. Tawk, Y. K. Yong, and A. J. Fleming, "3D-printed omnidirectional soft pneumatic actuators: Design, modeling and characterization," *Sensors and Actuators A: Physical*, vol. 332, p. 113199, Dec. 2021.
- [26] Z. Wang and S. Hirai, "A 3D printed soft gripper integrated with curvature sensor for studying soft grasping," in *2016 IEEE/SICE International Symposium on System Integration (SII)*, pp. 629–633, Dec. 2016. ISSN: 2474-2325.
- [27] O. D. Yirmibesoglu, J. Morrow, S. Walker, W. Gosrich, R. Cañizares, H. Kim, U. Daalkhaijav, C. Fleming, C. Branyan, and Y. Menguc, "Direct 3d printing of silicone elastomer soft robots and their performance comparison with molded counterparts," in *2018 IEEE International Conference on Soft Robotics (RoboSoft)*, pp. 295–302, 2018.
- [28] R. P. Rocha, P. A. Lopes, A. T. de Almeida, M. Tavakoli, and C. Majidi, "Fabrication and characterization of bending and pressure sensors for a soft prosthetic hand," *Journal of Micromechanics and Microengineering*, vol. 28, p. 034001, Jan. 2018.
- [29] B. Jamil, G. Yoo, Y. Choi, and H. Rodrigue, "Proprioceptive Soft Pneumatic Gripper for Extreme Environments Using Hybrid Optical Fibers," *IEEE Robotics and Automation Letters*, vol. 6, pp. 8694–8701, Oct. 2021. Conference Name: IEEE Robotics and Automation Letters.
- [30] T. Hellebrekers, O. Kroemer, and C. Majidi, "Soft Magnetic Skin for Continuous Deformation Sensing," *Advanced Intelligent Systems*, vol. 1, no. 4, p. 1900025, 2019. eprint: <https://onlinelibrary.wiley.com/doi/pdf/10.1002/aisy.201900025>.
- [31] A. B. Swanson, C. G. Hagert, and G. deGroot Swanson, "Evaluation of impairment of hand function," *The Journal of Hand Surgery*, vol. 8, pp. 709–722, Sept. 1983.
- [32] R. Deimel and O. Brock, "A novel type of compliant and underactuated robotic hand for dexterous grasping," *The International Journal of Robotics Research*, vol. 35, no. 1-3, pp. 161–185, 2016.
- [33] A. Kapandji, "Cotation clinique de l'opposition et de la contre-opposition du pouce," *Annales de Chirurgie de la Main*, vol. 5, pp. 67–73, Jan. 1986.
- [34] V. Sundaram, K. Ly, B. K. Johnson, M. Naris, M. P. Anderson, J. S. Humbert, N. Correll, and M. Rentschler, "Embedded Magnetic Sensing for Feedback Control of Soft HASEL Actuators," *IEEE Transactions on Robotics*, pp. 1–15, 2022. Conference Name: IEEE Transactions on Robotics.
- [35] T. Feix, I. M. Bullock, and A. M. Dollar, "Analysis of Human Grasping Behavior: Object Characteristics and Grasp Type," *IEEE Transactions on Haptics*, vol. 7, pp. 311–323, July 2014.
- [36] Y. Lin, A. S. Wang, G. Sutanto, A. Rai, and F. Meier, "Polymetis." <https://facebookresearch.github.io/fairo/polymetis/>, 2021.